Degeneracy of the 1/8 plateau and antiferromagnetic phases in the Shastry-Sutherland magnet TmB4

Trinh, Jennifer; Mitra, Sreemanta; Panagopoulos, Christos; Kong, Tai; Canfield, Paul C.; Ramirez, Arthur P.

2018

Trinh, J., Mitra, S., Panagopoulos, C., Kong, T., Canfield, P. C., & Ramirez, A. P. (2018). Degeneracy of the 1/8 plateau and antiferromagnetic phases in the Shastry-Sutherland magnet TmB4. Physical Review Letters, 121(16), 167203-. doi:10.1103/PhysRevLett.121.167203

https://hdl.handle.net/10356/106007

https://doi.org/10.1103/PhysRevLett.121.167203

Degeneracy of the 1/8 Plateau and Antiferromagnetic Phases in the Shastry-Sutherland Magnet TmB_4

Jennifer Trinh,[1] Sreemanta Mitra,[2,†] Christos Panagopoulos,[2] Tai Kong,[3,‡] Paul C. Canfield,[3] and Arthur P. Ramirez[1,*]

[1]*University of California Santa Cruz, Santa Cruz, California 95064, USA*

[2]*Division of Physics and Applied Physics, School of Physical and Mathematical Sciences, Nanyang Technological University, 637371, Singapore*

[3]*Ames Laboratory, Iowa State University, Ames, Iowa 50011, USA*

(Received 26 December 2017; published 18 October 2018)

The 1/8 fractional plateau phase (1/8 FPP) in Shastry-Sutherland lattice (SSL) spin systems has been viewed an exemplar of emergence on an Archimedean lattice. Here we explore this phase in the Ising magnet TmB_4 using high-resolution specific heat (C) and magnetization (M) in the field-temperature plane. We show that the 1/8 FPP is smoothly connected to the antiferromagnetic phase on ramping the field from $H = 0$. Thus, the 1/8 FPP is not a distinct thermodynamic ground state of TmB_4. The implication of these results for Heisenberg spins on the SSL is discussed.

DOI: 10.1103/PhysRevLett.121.167203

Magnetic systems with geometrically frustrated interactions [1,2] have produced a number of unconventional collective states, including spin ice [3], quantum spin liquid-like states [4], and fractional magnetization plateaus [5]. Although such states occur most commonly for short-range interactions on triangle-based crystal structures, when further-neighbor interactions are included, nontriangular lattices can also exhibit effects of frustration. One of most compelling examples of such frustration is that of antiferromagnetically interacting spins on the Shastry-Sutherland lattice (SSL). This lattice, isomorphic with the Archimedean lattice, was originally proffered for its exact ground state solution [6] and is realized in $SrCu_2(BO_3)_2$ [7,8] as well as in the RB_4 family, where R is a rare-earth element [9,10]. These SSL-containing compounds exhibit plateaus in the magnetization (M) at rational fractions (e.g., 1/2, 1/3, 1/8) of the saturation value (M_{sat}).

Whereas the experimental existence of plateaus in SSLs is firmly established, several different theoretical descriptions have been proposed. The fractional plateau phases (FPPs) in $SrCu_2(BO_3)_2$ have been described as crystals of triplon ($S = 1$) excitations [11–14] and, more recently, crystals of $S = 2$ bound states of triplons [15,16], the latter of which most accurately describes the observations. Another approach uses a mapping of spin operators to hard-core bosons and then to spinless fermions coupled to a Chern-Simons gauge field [17]. Recently, it has been shown that, in the presence of small interaction anisotropy, the triplons themselves form topological bands with Chern numbers ± 2 [18]. Among the FPPs that such theories need to replicate, the 1/8 FPP in particular has presented a puzzle. Small fractions such as 1/8 in a magnetic system, as well as in 2D electron gases, imply a high degree of correlation, which in turn places great demands on materials quality. While both the Heisenberg $SrCu_2(BO_3)_2$ as well as the Ising TmB_4 exhibit this phase in both thermodynamic [7,8,19–27] as well as probes of local order [24,28], it is not reproduced by every theory. For example, while some theories reproduce the 1/8 FPP for $SrCu_2(BO_3)_2$ [17,29–32], the Chern-Simons mapping does not. More generally, analytic theories of the FPPs treat them as distinct phases, stabilized by either a crystal formation energy or a topological principle. One might argue that the observation of FPPs of similar fractions in both Heisenberg and Ising systems with vastly different energy scales and ranges of interaction suggests a shared origin. Thus, in order to discuss these phases in a materials-agnostic way, it is imperative that their experimental stability be firmly established.

Here, we investigate the 1/8 FPP region in TmB_4 using both magnetization and specific heat (C). This metallic, tetragonal ($P4/mbm$), quasi-2D compound has Ising-like effective spins (Tm^{3+}, $J = 6$ non-Kramers doublet) interacting primarily via Ruderman-Kittel-Kasuya-Yosida indirect exchange. The magnetic field (H) versus temperature (T) phase diagram has been studied with M [22,23,26], C [23,25], neutron diffraction [24], and charge transport [27], and the major features are shown in the inset of Fig. 1. The 1/8 FPP appears as a narrow region in the H-T plane between $H = 1.40$ and 1.75 T, and hysteresis in the value of the M in the plateau region, as opposed to the location of its boundaries, is seen. In this region, Siemensmeyer *et al.* [24] and Wierschem *et al.* [26] observe M/M_{sat} fractions of 1/7, 1/9, and 1/11, in addition to 1/8. By performing complementary measurements of C and M using the same H-T sweep protocols, we address the thermodynamic nature of the 1/8 FPP. We find hysteresis

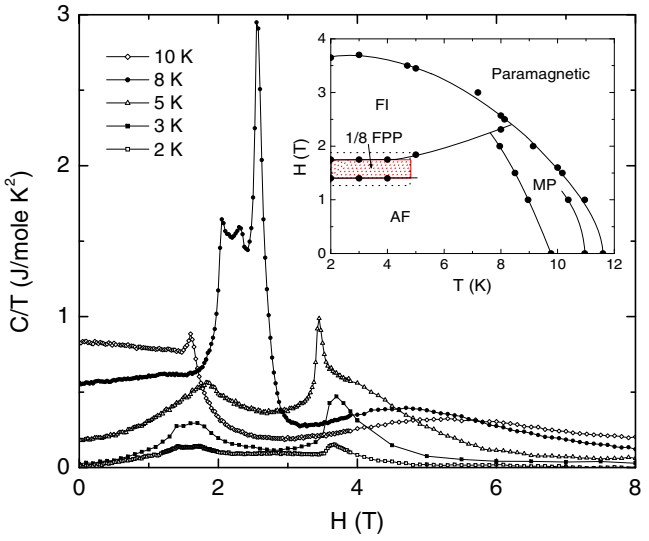

FIG. 1. Specific heat divided by temperature C/T as a function of magnetic field H, for various values of fixed T. (Inset) Phase boundary as determined from these measurements, as well as those of C/T versus T at fixed H (available in Supplemental Material [33]) showing the AF, FI, mixed phase (MP), and 1/8 FPP.

in $C(H)$ around the FPP region, suggesting a dynamical origin of this phase. More importantly, we find that, on approaching the 1/8 FPP region from $H = 0$, it is possible to enter this region from the antiferromagnetic (AF) state without crossing a phase line. This result suggests that the 1/8 FPP is either not symmetry distinct from the AF phase or that the transition proceeds through other nearly degenerate long-wavelength states. Such near degeneracy of states may help to explain why the 1/8 FPP has been difficult to reproduce theoretically.

The 0.28 mg crystal used here was grown from solution using a technique described elsewhere [26]. Measurements of M were obtained with a commercial SQUID magnetometer. For measurements of C, the sample was mounted with silicone grease on a small copper block, which became part of the addendum, and all such data were obtained using the thermal relaxation technique. Measurements of both M and C were performed with H along the c axis, i.e., normal to the 2D planes. In this direction, the demagnetization factor is $4\pi(0.15 \pm 0.02)$ for our sample, whose $a:b:c$ dimensions are 0.30:0.30:0.65 mm [34]. The protocol used for the measurements used to compare M and C was to (1) cool the sample to a temperature T with $H = 0$, (2) ramp H to 5 T, where $M = M_{\mathrm{sat}}$, (3) ramp H to 2 T, (4) obtain data (either M or C) on ramping H down, (5) ramp H to 0 and back up to 1.4 T, and (6) obtain data on ramping H up to 2 T. By performing both M and C measurements on the same sample with the same protocol, the features associated with the FPP region can be faithfully compared.

In Fig. 1, we show $C(H)$ for different values of T encompassing the entire phase diagram, shown in the inset. Additional points on the diagram came from measurements at fixed H, the data of which are available in the Supplemental Material [33]. The ordering features are more clearly defined than in previous $C(H)$ measurements [25], suggesting high sample quality. In the following, we will focus on the region of the phase diagram enclosed by a dotted rectangle in the phase diagram.

In Fig. 2, we show $C(H)$ and $M(H)$ for six different temperatures encompassing the 1/8 FPP. Similar to previous studies, we observe jumps in $M(H)$ centered at 1.40 and 1.75 T. These jumps are spread out over small regions of external field H, and thus are consistent with first-order transitions as a function of the internal field H_i. In such a case, $\chi^{-1} = (\partial M/\partial H)^{-1} = N$, where N is the demagnetization factor, in the regions where M is increasing. Using $M_{\mathrm{sat}} = 7\ \mu_B$, we find that $\chi^{-1} = 4\pi(0.166)$, which is within experimental error for the estimated demagnetization factor of our sample. This suggests that the narrow regions where M is rapidly changing are mixed phases of the 1/8 FPP with the AF phase ($0.138 < H < 0.143$ T) and the ferrimagnetic (FI) phase ($1.73 < H < 1.81$ T). In the following, we present M and C as a function of external field H. The demagnetization correction for C itself will be greatest in the transition regions [35]. Such a correction is only meaningful, however, for a uniform H_i and absent domain structure. As we show below, such assumptions are likely not valid in the 1/8 FPP region, and thus we will discuss C as a function of H with no loss of generality, but realizing the observed peaks will likely be sharper when expressed in terms of H_i.

In Fig. 2, at the lowest and highest temperatures, we see two limiting behaviors. At 2.0 K [Fig. 2(f)], the transition from AF to FI states proceeds via two distinct and nearly reversible transitions. The step in magnetization, from $M/M_{\mathrm{sat}} \approx 0$ to $M/M_{\mathrm{sat}} \approx 1/8$ in the 1/8 FPP at $H = 1.40$ T is accompanied by a corresponding peak in C/T, as expected for a thermodynamic transition. As alluded to above, a distinction should be drawn between a magnetization-reversal process occurring, e.g., in a hard ferromagnet and a thermodynamic transition, i.e., one involving a thermodynamic number of spins. The former involves virtually no change in the local spin configuration and would not necessarily be accompanied by a corresponding peak in $C(H)$, whereas the latter involves reconfiguration of local spin textures at interatomic spacings and would be signaled by a peak in $C(H)$. At 2.0 K, $C(H)$ provides evidence that the $M(H)$ step is indeed a thermodynamic transition. Similarly, at $H = 1.75$ T, M/M_{sat} jumps up to 0.5 on entering the FI state, accompanied by another peak in C/T. The signatures of these two transitions are virtually the same on increasing and decreasing magnetic field, indicating that microscopic statistical processes are governing the macroscopic response.

The behavior at $T = 4.5$ K [Fig. 2(a)] is qualitatively different from that at 2.0 K. Whereas for increasing H, the

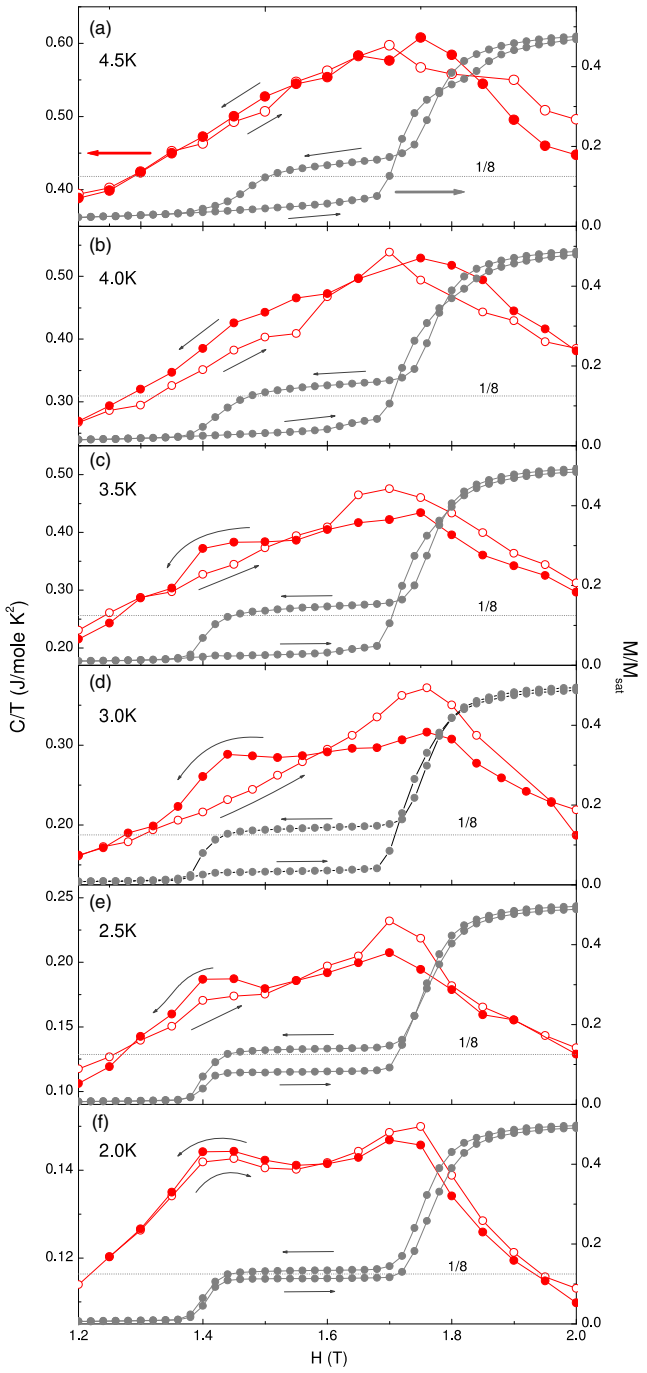

FIG. 2. Specific heat divided by temperature C/T and magnetization M as a function of magnetic field H, for various temperatures encompassing the FPP. The field sweep protocol is discussed in the text. Date in frames (a)–(f) were obtained at temperatures from 4.5–2.0K, as indicated in the frames.

ordering features in C/T and $M/M_{\rm sat}$ are observed only at $H \approx 1.75$ T, for decreasing H, an additional jump down in $M/M_{\rm sat}$ at $H = 1.47$ T is observed but not accompanied by a corresponding peak in C/T. Thus, while a plateau in $M(H)$ has developed, this behavior is not mirrored in $C(H)$. We note that the temperature difference between 2.0 and 4.5 K is large in relative terms and that for $H = 1.3$ T

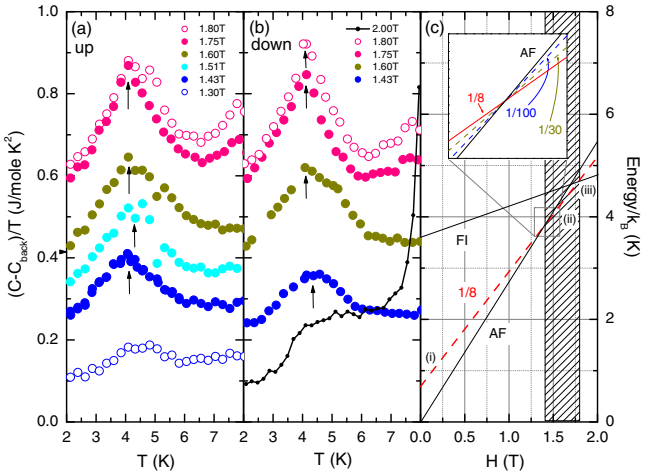

FIG. 3. (a) Specific heat divided by temperature C/T, with a linear background term $C_{\rm back} = 0.083(T-2)$ subtracted, versus temperature taken on increasing temperature, showing a peak that defines the high-temperature boundary of the FPP region. The data have also been offset by adding a constant equal to (H-1.3). (b) Same as (a), but data taken on cooling. (c) Energy level diagram at zero temperature, as dictated by the positions of the phase boundaries via criteria i–iii as discussed in the text. (Inset) Schematic of the expected energy levels of $M/M_s < 1/8$ plateau states.

(just below the 1.40 T step) $M/M_{\rm sat} = 8.2 \times 10^{-3}$ at 2.0 K and 2.8×10^{-3} at 4.5 K. Thus, at 4.5 K, the number of spin-flip processes available for rearranging magnetic order is almost 3 times larger than at 2.0 K.

We gain insight into the processes governing the transition out of the $1/8$ FPP from the behavior between 2.5 and 4.0 K, shown in Figs. 2(b)–2(e). For field up sweeps, the plateau value of $M/M_{\rm sat}$ decreases from 0.114 (2.0 K) to 0.027 (3.5 K), a factor of 4.2. On field down sweeps, however, the behavior is qualitatively different. In the same range of T, $M/M_{\rm sat}$ changes from 0.134 (2.0 K) to 0.154 (4.5 K), only a 14% increase. Thus, the hysteresis loop in $M/M_{\rm sat}$ opens up as temperature is increased, an effect that results primarily from the reduction of magnetization on field up sweep. The data in Figs. 2(d)–2(f) show that this reduction in $M/M_{\rm sat}$ is accompanied by the vanishing of critical behavior in C/T on up sweep at $H = 1.40$ T. Whereas on down sweep, $M/M_{\rm sat}$ exhibits little change in the 1.40 T jump over the entire temperature region, the critical response of C/T on down sweep vanishes with increasing T. Thus, we see that different protocols by which the $1/8$ FPP is approached yield qualitatively different pictures of its lower field boundary.

As seen in Fig. 2, the $C(H)$ data change dramatically between 2.0 and 4.5 K, suggesting the presence of a T constant phase boundary. In order to define this phase boundary, we performed $C(T)$ measurements at several values of fixed H, for both increasing and decreasing T, as shown in Figs. 3(a) and 3(b), respectively. Indeed, we see sharp ordering features at $T \sim 4.2$ K for H values that

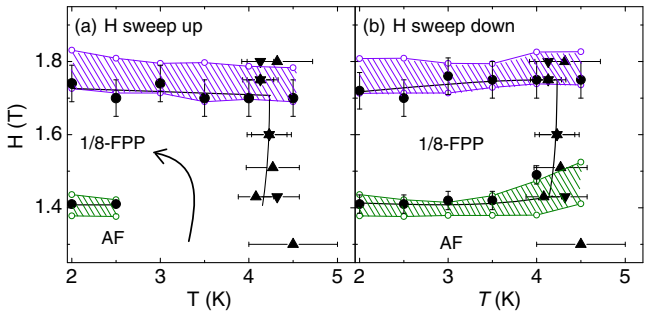

FIG. 4. The phase diagram around the 1/8 FPP as determined by specific heat measurements, denoted by solid black symbols. The circles are obtained from $C(H)$ in Fig. 2 and the up (down) triangles denote the peaks in $C(T)$ shown in Fig. 3(a) [Fig. 3(b)]. The solid lines are guides to the eye. (a) Sweeping up in field—The low (high) field hatched regions are mixed 1/8 FPP/AF(FI) phases, as expected for first-order transitions, defined by $M(H)$ measurements shown in Fig. 2. The curved arrow shows a possible route for entering the 1/8 FPP from the AF phase without crossing a phase boundary. (b) Sweeping down in field—The hatched regions are defined as in (a).

bracket the 1/8 FPP. Both above (2.0 T) and below (1.3 T) the 1/8 FPP region, the peaks broaden into a short-range-order feature. Thus, we observe a T constant phase boundary, not previously reported, that, along with the H constant boundaries at 1.41 and 1.75 T, fully delineate the 1/8 FPP region on H down sweeps.

The phase boundaries obtained around the 1/8 FPP region as defined by $C(T,H)$ are shown in Fig. 4. While the 1/8 FPP region is now well defined, it is only bounded and distinct from the AF phase with decreasing H. When data are obtained on increasing H, a gap in the boundary is seen between $T = 2.5$ and $T = 4.0$ K, allowing paths from the AF to 1/8 FPP regions without a thermodynamic ordering feature. Thus, it is likely that the presence of other FPPs, indicated by the seemingly continuous reduction of M in this region on increasing H, leads to the traversal of a sequence of nearly degenerate phases en route from the AF to the 1/8 FPP region. This situation is akin to the critical point of water, around which exist paths in the pressure-temperature plane that allow the conversion from gas to liquid without traversing a critical line. On sweeping down in field, the system must transform from the FI state, in which ½ of the spins are fully aligned, to the 1/8 FPP. This dramatic reorientation of spins presumably creates the dynamic phase space for selecting the lowest energy 1/8 FPP.

A simple state-energy analysis reveals why the AF, 1/8 FPP, and other fractional FPPs are nearly degenerate between 1.41 and 1.75 T. Following Tinkham's [36] treatment of the metamagnet $CoCl_2 \cdot 2H_2O$, and using the ordered patterns reported by Siemensmeyer *et al.* [24] for the AF and FI phases of TmB_4, we equate the $T = 0$ energy of the AF and FI phases at $H_{c1} = 1.5$ T, and the FI and paramagnetic (fully polarized at $T = 0$) phases at $H_{c2} = 3.7$ T. This yields values for the SSL nearest-neighbor exchange interactions of $J_1 = 0.45$ and $J_2 = 1.25$ K, assuming an effective spin of 6, producing an energy difference of $3.6k_B$ between the AF and FI states at $H = 0$, as shown in Fig. 3(c). We know that the FI and AF state energies (E) must obey $dE/dH > 0$, and we make the reasonable assumptions i) that $E(1/8\ \mathrm{FPP})$ is greater than $E(\mathrm{AF})$ at $T = 0$, $H = 0$, ii) that $E(1/8\ \mathrm{FPP}) = E(\mathrm{AF})$ at $H = 1.41$ T, and iii) that $E(1/8\ \mathrm{FPP}) > E(\mathrm{FI})$ for $H > 1.75$ T. These constraints dictate a $T = 0$ energy level diagram similar to that shown in Fig. 3(c). Increasing T will reduce the energy differences but not substantively change the constraint conditions, as evidenced by the negligible dependence of H_{c1} and H_{c2} on T. We see, therefore, that the difference in energy between the AF and 1/8 FPP is only a few tenths of a Kelvin and cannot change significantly for different dE/dH values, given the above constraints. The 1/8 FPP is created from the AF state by flipping 1/16 of the spins. The plateaus with $M/M_s < 1/8$ observed on up field sweeps are created with even fewer spin flips. For example, the plateau seen for $T = 3.0$ K in Fig. 2(d) has $M/M_s = 1/30$, which is obtained by flipping 1/60 of the spins. The near degeneracy of these states is shown schematically in the inset of Fig. 3(c).

We have shown that the 1/8 FPP can be accessed via the AF state in a manner similar to the triple point of water. We have also shown that $M(T,H)$ in the 1/8 FPP region can adopt a seemingly continuous set of values in H up sweeps. These observations lead us to conclude that the 1/8 FPP is not a thermodynamically stable state, but rather a metastable variant on the AF state created on approaching the phase boundary to the 1/2 FPP. This result has important ramifications for the study of magnetization plateaus. First, it shows that an observed fractional magnetization should not be construed as a stable ground state of the system. Thus, the inability of the Chern-Simons mapping for $SrCu_2(BO_3)_2$ to reproduce the 1/8 FPP might not necessarily be a failure of the theory. Second, plateau phases need to be reconciled with the complete phase diagram. The type of study presented here will be difficult to perform on $SrCu_2(BO_3)_2$ given that the 1/8 FPP occurs at the high field of $H = 27$ T, but the present Letter provides motivation to pursue such work. Finally, among quantum spin liquids that admit non-Abelian excitations, FPP states are good candidates for in-depth studies. The present Letter shows that, in order to even begin a search for such excitations, phase stability needs to be established.

This work was supported by the U.S. National Science Foundation Grant No. NSF-DMR 1534741 (J. T.), U.S. Department of Energy Grant No. DE-SC0017862 (A. P. R.), Ministry of Education, Singapore MOE2014-T2-2-112 (S. M. and C. P.), and the Singapore National Research Foundation, Investigatorship NRF-NRFI2015-04 (S. M. and C. P.). Work at Ames Lab (P. C. C. and T. K.) was supported by the U.S. Department of Energy, Office of Basic Energy Science, Division of Materials Sciences and

Engineering. Ames Laboratory is operated for the U.S. Department of Energy by Iowa State University under Contract No. DE-AC02-07CH11358. We would also like to thank Sriram Shastry and Steve Simon for helpful insights.

*Corresponding author.
apr@ucsc.edu
†Present address: Department of Physics, Indian Institute of Science, Bangalore, 560012, India.
‡Present address: Department of Chemistry, Princeton University, Princeton New Jersey, 08544, USA.

[1] G. H. Wannier, Antiferromagnetism. The triangular Ising net, Phys. Rev. **79**, 357 (1950).
[2] A. P. Ramirez, Strongly geometrically frustrated magnets, Annu. Rev. Mater. Sci. **24**, 453 (1994).
[3] A. P. Ramirez, A. Hayashi, R. J. Cava, R. Siddharthan, and B. S. Shastry, Zero-point entropy in "spin ice", Nature (London) **399**, 333 (1999).
[4] J. S. Helton, K. Matan, M. P. Shores, E. A. Nytko, B. M. Bartlett, Y. Yoshida, Y. Takano, A. Suslov, Y. Qiu, J. H. Chung, D. G. Nocera, and Y. S. Lee, Spin Dynamics of the Spin-1/2 Kagome Lattice Antiferromagnet $ZnCu_3(OH)_6Cl_2$, Phys. Rev. Lett. **98**, 107204 (2007).
[5] T. Sakakibara, T. Tayama, Z. Hiroi, K. Matsuhira, and S. Takagi, Observation of a Liquid-Gas-Type Transition in the Pyrochlore Spin Ice Compound $Dy_2Ti_2O_7$ in a Magnetic Field, Phys. Rev. Lett. **90**, 207205 (2003).
[6] B. S. Shastry and B. Sutherland, Exact ground-state of a quantum-mechanical antiferromagnet, Physica (Amsterdam) **108B+C**, 1069 (1981).
[7] H. Kageyama, K. Onizuka, Y. Ueda, N. V. Mushnikov, T. Goto, K. Yoshimura, and K. Kosuge, Magnetic anisotropy of $SrCu_2(BO_3)_2$ with a two-dimensional orthogonal dimer lattice, J. Phys. Soc. Jpn. **67**, 4304 (1998).
[8] H. Kageyama, K. Yoshimura, R. Stern, N. V. Mushnikov, K. Onizuka, M. Kato, K. Kosuge, C. P. Slichter, T. Goto, and Y. Ueda, Exact Dimer Ground State and Quantized Magnetization Plateaus in the Two-Dimensional Spin System $SrCu_2(BO_3)_2$, Phys. Rev. Lett. **82**, 3168 (1999).
[9] S. Michimura, A. Shigekawa, F. Iga, M. Sera, T. Takabatake, K. Ohoyama, and Y. Okabe, Magnetic frustrations in the Shastry-Sutherland system ErB_4, Physica (Amsterdam) **378B**, 596 (2006).
[10] S. Yoshii, T. Yamamoto, M. Hagiwara, T. Takeuchi, A. Shigekawa, S. Michimura, F. Iga, T. Takabatake, and K. Kindo, High-field magnetization of TbB_4, J. Magn. Magn. Mater. **310**, 1282 (2007).
[11] S. Miyahara and K. Ueda, The magnetization plateaus of SrCu2(BO3)(2), Physica (Amsterdam) **281B**, 661 (2000).
[12] S. Miyahara and K. Ueda, Superstructures at magnetization plateaus in SrCu2(BO3)(2), Phys. Rev. B **61**, 3417 (2000).
[13] T. Momoi and K. Totsuka, Magnetization plateaus of the Shastry-Sutherland model for SrCu2(BO3)(2): Spin-density wave, supersolid, and bound states, Phys. Rev. B **62**, 15067 (2000).
[14] T. Momoi and K. Totsuka, Magnetization plateaus as insulator-superfluid transitions in quantum spin systems, Phys. Rev. B **61**, 3231 (2000).
[15] P. Corboz and F. Mila, Crystals of Bound States in the Magnetization Plateaus of the Shastry-Sutherland Model, Phys. Rev. Lett. **112**, 147203 (2014).
[16] Z. T. Wang and C. D. Batista, Dynamics and Instabilities of the Shastry-Sutherland Model, Phys. Rev. Lett. **120**, 247201 (2018).
[17] G. Misguich, T. Jolicoeur, and S. M. Girvin, Magnetization Plateaus of $SrCu_2(BO_3)_2$ from a Chern-Simons Theory, Phys. Rev. Lett. **87**, 097203 (2001).
[18] J. Romhányi, K. Penc, and R. Ganesh, Hall effect of triplons in a dimerized magnet, Nat. Commun. **6**, 6805 (2015).
[19] K. Onizuka, H. Kageyama, Y. Narumi, K. Kindo, Y. Ueda, and T. Goto, 1/3 magnetization plateau in $SrCu_2(BO_3)_2$—Stripe order of excited triplets, J. Phys. Soc. Jpn. **69**, 1016 (2000).
[20] F. Levy, I. Sheikin, C. Berthier, M. Horvatic, M. Takigawa, H. Kageyama, T. Waki, and Y. Ueda, Field dependence of the quantum ground state in the Shastry-Sutherland system $SrCu_2(BO_3)_2$, Europhys. Lett. **81**, 67004 (2008).
[21] H. Tsujii, C. R. Rotundu, B. Andraka, Y. Takano, H. Kageyama, and Y. Ueda, Specific heat of the $S = 1/2$ two-dimensional Shastry-Sutherland antiferromagnet $SrCu_2(BO_3)_2$ in high magnetic fields, J. Phys. Soc. Jpn. **80**, 043707 (2011).
[22] F. Iga, A. Shigekawa, Y. Hasegawa, S. Michimura, T. Takabatake, S. Yoshii, T. Yamamoto, M. Hagiwara, and K. Kindo, Highly anisotropic magnetic phase diagram of a 2-dimensional orthogonal dimer system TmB4, J. Magn. Magn. Mater. **310**, E443 (2007).
[23] S. Gabani, S. Matas, P. Priputen, K. Flachbart, K. Slemensmeyer, E. Wulf, A. Evdokimova, and N. Shitsevalova, Magnetic structure and phase diagram of TmB_4, Acta Phys. Pol. A **113**, 227 (2008).
[24] K. Siemensmeyer, E. Wulf, H. J. Mikeska, K. Flachbart, S. Gabani, S. Mat'as, P. Priputen, A. Efdokimova, and N. Shitsevalova, Fractional Magnetization Plateaus and Magnetic Order in the Shastry-Sutherland Magnet TmB_4, Phys. Rev. Lett. **101**, 177201 (2008).
[25] J. Kacmarcik, Z. Pribulova, S. Gabani, P. Samuely, K. Siemensmeyer, N. Shitsevalova, and K. Flachbart, Phase diagram of TmB_4 probed by ac calorimetry, Acta Phys. Pol. A **118**, 903 (2010).
[26] K. Wierschem, S. S. Sunku, T. Kong, T. Ito, P. C. Canfield, C. Panagopoulos, and P. Sengupta, Origin of modulated phases and magnetic hysteresis in TmB_4, Phys. Rev. B **92**, 214433 (2015).
[27] S. S. Sunku, T. Kong, T. Ito, P. C. Canfield, B. S. Shastry, P. Sengupta, and C. Panagopoulos, Hysteretic magnetoresistance and unconventional anomalous Hall effect in the frustrated magnet TmB_4, Phys. Rev. B **93**, 174408 (2016).
[28] M. Takigawa, S. Matsubara, M. Horvatc, C. Berthier, H. Kageyama, and Y. Ueda, NMR Evidence for the Persistence of a Spin Superlattice beyond the 1/8 Magnetization Plateau in $SrCu_2(BO_3)_2$, Phys. Rev. Lett. **101**, 037202 (2008).
[29] S. E. Sebastian, N. Harrison, C. D. Batista, L. Balicas, M. Jaime, P. A. Sharma, N. Kawashima, and I. R. Fisher, Dimensional reduction at a quantum critical point, Nature (London) **441**, 617 (2006).

[30] J. Dorier, K. P. Schmidt, and F. Mila, Theory of Magnetization Plateaux in the Shastry-Sutherland Model, Phys. Rev. Lett. **101**, 250402 (2008).

[31] A. Abendschein and S. Capponi, Effective Theory of Magnetization Plateaux in the Shastry-Sutherland Lattice, Phys. Rev. Lett. **101**, 227201 (2008).

[32] M. Nemec, G. R. Foltin, and K. P. Schmidt, Microscopic mechanism for the $1/8$ magnetization plateau in $SrCu_2(BO_3)_2$, Phys. Rev. B **86**, 174425 (2012).

[33] See Supplemental Material at http://link.aps.org/supplemental/10.1103/PhysRevLett.121.167203 for C/T versus T at fixed H for the sample studied in this work.

[34] J. A. Osborn, Demagnetizing factors of the general ellipsoid, Phys. Rev. **67**, 351 (1945).

[35] P. M. Levy and D. P. Landau, Shape dependence of specific heat of magnetic systems with long-range interactions, J. Appl. Phys. **39**, 1128 (1968).

[36] M. Tinkham, Microscopic dynamics of metamagnetic transitions in an approximately Ising system. $CoCl_2 \cdot 2H_2O$, Phys. Rev. **188**, 967 (1969).